Heat flows through plasma sheaths*

S. Takamura,[†,a)] M. Y. Ye, T. Kuwabara, and N. Ohno
Department of Energy Engineering and Science, Graduate School of Engineering, Nagoya University, Nagoya 464-01, Japan

(Received 19 November 1997; accepted 8 December 1997)

Plasma heat flow to material surfaces through sheaths is studied, taking several key physics factors into account. Electron emission from the surface, which breaks a thermal insulation of the sheath, is studied in both thermoelectron emission (TEE) and secondary electron emission (SEE), in which a correct expression under space charge limited condition is given for arbitrary sheath voltages. Nonlinear thermal bifurcation induced by electron emission is analyzed in the experiment and the theory. The local heat flow was found to be enhanced by a thermal contraction induced by cross-field potential variation in a plasma. An enhancement of SEE of hydrogen-absorbed graphite, and a suppression of SEE by the gyromotion of emitted electrons in obliquely incident magnetic field are identified. The effects of ion reflection on the surface and ponderomotive force are also discussed in terms of energy transmission factor δ. An anomaly of δ in detached recombining plasmas is discussed. © *1998 American Institute of Physics.* [S1070-664X(98)90705-4]

I. INTRODUCTION

Plasma heat flow to material surfaces critically depends on the characteristics of the plasma sheath located between the plasma and the material surface. Recently, it has become crucially important for divertor physics in magnetic fusion devices. It also has an important role in magnetohydrodynamic (MHD) generators, arc plasmas, and the re-entry of space vehicles into the atmosphere. However, it has never been studied systematically in a comprehensive way.[1] Here, we would like to describe the key physics factors determining heat flows to material surfaces through plasma sheaths.

There are several key factors which determine the energy transmission through the sheath. The most important one is the electron emission from the material surface, either thermoelectron emission (TEE) or secondary electron emission (SEE), because the sheath voltage (SV), which is a potential barrier for incoming plasma electrons, would be greatly reduced by it so that the thermal insulation may become substantially low. The emission current may be regulated by space charge effect in the sheath. However, it has never been given in an explicit form for arbitrary SV. SEE is enhanced by surface contamination; for example, hydrogen in graphite, and grazing incidence of primary electrons. It is, on the other hand, suppressed by the gyromotion of emitted electrons in an obliquely incident magnetic field. The other physical processes influencing the energy transmission through the sheath are the ion reflection on the material surface, and the ponderomotive force (PF). The latter modifies the sheath and the presheath. Several nonlinear phenomena are associated with the above-mentioned physical processes: Bifurcation due to nonlinear relation of electron emission to the heat flow on the material surface, thermal contraction induced by cross-field plasma potential variation, leading to a kind of hot spot formation.

In the next section, we briefly summarize the present understanding of the energy transmission through plasma sheaths in terms of energy transmission factor δ. The third section is mainly devoted to the precise expression of space charge limited current through the plasma sheath. Using this expression, the nonlinear bifurcation phenomena, as well as thermal contraction, are formulated, and compared with experimental results. The enhancement and suppression of SEE are also shown in the same section. Experimental observation of δ reduction due to ion reflection will be reported in the fourth section in which the theory on sheath or presheath modification by PF will be given and some related experiments will be pointed out. In addition, the effect of collisions in the sheath on δ is discussed in relation to the accurate measurement of plasma parameters near the material surface. Some conclusions and remaining problems will be given in the final section.

II. ENERGY TRANSMISSION FACTOR

We define δ as a function of SV, ϕ, by the ratio of the plasma heat flux $q(\phi)$ onto the material surface to the electron temperature T_e times the normal ion particle flux $j_{is}^{+}/e = n_{se}C_s$:

$$\delta(\phi) \equiv \frac{q(\phi)}{T_e(j_{is}^{+}/e)} = \frac{2T_i + 0.5(T_e+T_i)M^2 - e\phi}{T_e}(1-R_{ie})M + \frac{e\phi_i}{T_e}M + 2\left[\left(1+\frac{T_i}{T_e}\right)\left(\frac{2\pi m_e}{m_i}\right)\right]^{-1/2} e^{\Phi}, \quad (1)$$

where R_{ie} is the energy reflection coefficient of incident ions, ϕ_i is the ionization potential, Φ is the normalized sheath

*Paper g TuaI 2-4 Bull. Am. Phys. Soc. **42**, 1877 (1997).
[†]Invited speaker.
[a)]Electronic mail: takamura@nuee.nagoya-u.ac.jp

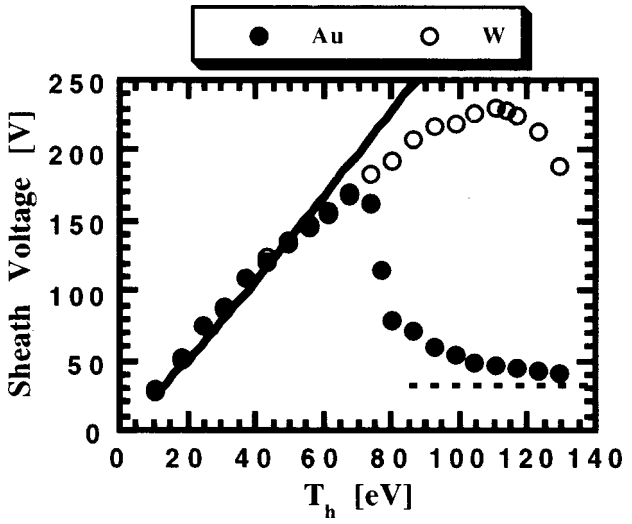

FIG. 1. Dependences of SV on the effective parallel temperature of hot electrons. Solid line shows theoretical formula, Eq. (3), without SEE, where α is assumed 0.5. Dotted line is theoretically obtained by the floating condition using the correct expression for space charge limited current, Eq. (5).

voltage $e\phi/T_e$, and M and n_{se} are the Mach number of ion flow velocity and the plasma density at the sheath edge. The latter is related to the upstream plasma density by $n_0 = 2n_{se}$. The first term comes from the ionic kinetic energy, the second one is the surface recombination energy, and the last term represents the electron kinetic energy.

The plasma sheath has intrinsically the role of thermal insulation of plasmas from the surrounding material surface. The SV dependence of δ gives a minimum at close to the floating voltage. The ion reflection decreases the incident energy by $1-R_{ie}$. Even when the plasma is very cold, the residual energy release on the surface due to surface recombination becomes substantial when the ion flux to the surface is large as is encountered in a divertor target plate in reactor-sized tokamaks,[2] where the conservation of plasma pressure along the magnetic-field line makes an increase in plasma density when the plasma is cooled down.[3] It makes a requirement of decrease in ion flux due to volumetric recombination in plasmas.[4]

The electron emission decreases the SV, which increases exponentially the electron incident energy due to the diminution of potential barrier for plasma electrons. If we have a rapidly oscillating electric field in the sheath or the presheath, the ponderomotive potential may be added to the electrostatic potential, so that the electron influx to the surface may be modified. Another factor influencing δ would be an ion-neutral collision in the sheath.

III. ELECTRON EMISSION FROM THE SURFACE

A. Secondary electron emission

Nonisothermal plasma ($T_e \gg T_i$) gives the following SV

$$\phi = \frac{T_e}{e} \ln\left(M\sqrt{\frac{2\pi m_e}{m_i}} + \frac{j_{em}^-}{(en_{se}/4)\sqrt{8T_e/\pi m_e}} \right), \qquad (2)$$

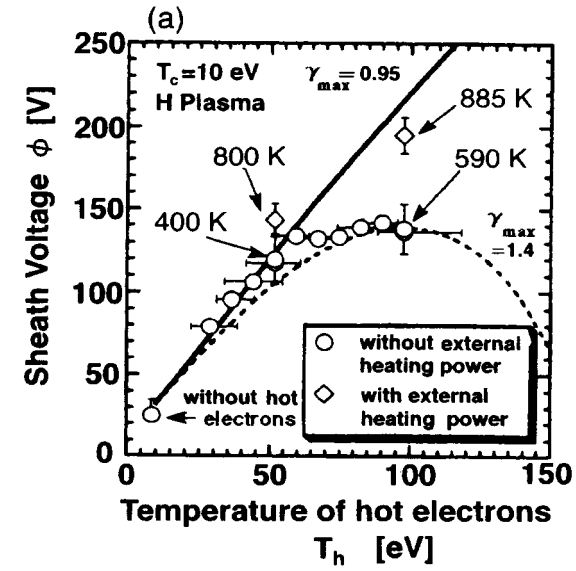

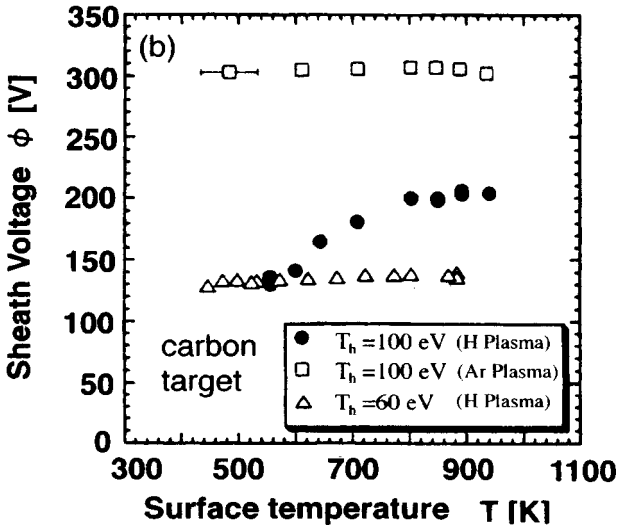

FIG. 2. (a) Comparison of observed SV at low and high target temperatures with those theoretically obtained for pure carbon (solid line; $\gamma_{max}=0.95$ at $E=400$ eV) and for an enhanced yield (dashed line, $\gamma_{max}=1.4$ due to hydrogen absorption). (b) Dependences of SV on the carbon surface temperature in H_2 and Ar plasmas.

where j_{em}^- is the electron emission current from the surface. The SV is proportional to T_e. This proportionality is still valid when we have two components, bulk electrons T_e and hot electrons T_h, if the hot electron abundance α satisfies the condition, $\alpha > (T_{\rm eff}/T_h)^{1/2}(2\pi m_e/m_i)^{[1-(T_{\rm eff}/T_h)]/2}$:

$$\phi = \frac{T_h}{e} \ln\left[\frac{1}{\alpha(1-\gamma)} \left(\frac{T_{\rm eff}}{T_h} \frac{2\pi m_e}{m_i} \right)^{1/2} \right], \qquad (3)$$

where γ is the SEE yield and $T_{\rm eff}$ is defined by $T_{\rm eff}^{-1} = (1-\alpha)T_c^{-1} + \alpha T_h^{-1}$. Figure 1 shows the experimentally observed SV, compared to Eq. (3) with $\gamma = 0$.[5] A fairly good agreement is obtained in the energy range with no SEE. The SV drops gradually in tungsten and rapidly in gold, depending on each SEE yield. In the case of Au the space charge limited SEE current gives a very low voltage almost independent of T_h, which will be discussed in the next subsec-

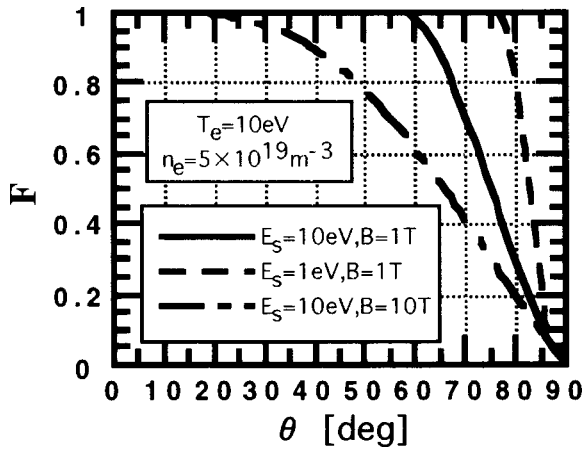

FIG. 3. Dependence of the angle θ on F when the structure of the electrostatic and magnetic sheaths is taken into account.

tion. Instead of metal, graphite, popular as a material for the first wall in fusion devices, has a rather complicated behavior as shown in Fig. 2. The hydrogen absorption gives a substantial increase in SEE due to the reduction of required energy to make secondary electrons in the solid by the cascade process by more than a factor of 2 for hydrogen atom compared with carbon.[6] The hydrogen contribution to SEE was confirmed either by removing hydrogen from the graphite with an increase in the surface temperature or by testing in hydrogen-free argon plasma.[7]

The SEE is governed by the gyromotion of electrons emitted from the surface having a grazing incident magnetic field. It makes the emitted electrons return to the surface, although the sheath electric field **E** makes those electrons go away from the surface and might break down the suppression of SEE. Concerning the emission fraction F, over the parameter range in which F changes rapidly, F is proportional to the ratio of electrostatic to Lorentzian forces, or the ratio of $\mathbf{E}\times\mathbf{B}$ velocity to the emission velocity. F is plotted as a function of the angle θ between the magnetic-field line and the surface normal in Fig. 3.[8] Detailed angular dependence of observed SV for Au and W target plates are, respectively, represented in Figs. 4(a) and 4(b). At the T_h below 65 eV, the voltage is almost the same for both materials where there are slow decreases of ϕ with θ from 0° toward $\pm 90°$, indicating the decrement of electron current compared with the ion current due to the decrease of effective perpendicular surface area $S\cos\theta$. The ion current does not decrease as much with θ, owing to the finite Larmor radius. In a middle range of T_h, 80–100 eV for W, a sharp drop in the voltage with angle is attributed to the increase of γ by the oblique incidence of primary electrons to the target. This is very much pronounced in T_h of 75 eV for Au and 115 eV for W. We note that a small increase in ϕ is observed at θ close to 90°, showing the suppression of SEE. The peak becomes very clear at $T_h=100$ eV for Au, where the suppression of SEE overcomes the enhancement of SEE due to the oblique incidence of primary electrons.

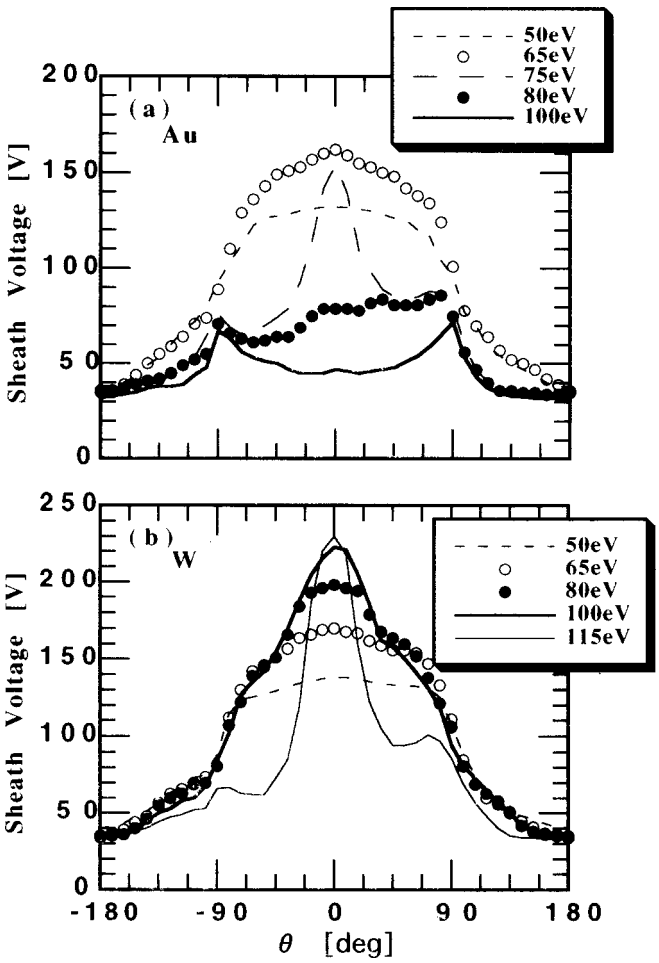

FIG. 4. Dependences of SV on the angle θ for (a) Au and (b) W targets taking effective parallel temperature of hot electrons T_h as a parameter.

B. Space-charge limited current

The space-charge limited current in vacuum is described by the following Child–Langmuir (CL) expression: $j_{\mathrm{CL}}=(4\varepsilon_0/9)(2e/m_e)^{1/2}\phi^{1.5}/d^2$, where d is the distance between two electrodes. If we apply CL equation in a plasma, d could be a sheath thickness which is a few times the Debye length: $d=k\lambda_{De}$.[9] It gives

$$j_{\mathrm{CL}}=\frac{4n_{se}e}{9k^2}\left(\frac{2T_e}{m_e}\right)^{1/2}\Phi^{3/2}. \tag{4}$$

In the electrically floated condition, the modified CL expression gives a floating SV given by Hobbs and Wesson when we employ $k=2.2$.[10] This is confirmed by one-dimensional particle simulation, giving $k=2.0$–2.6.[11] Equation (4) has been successfully employed to explain the SV under the following space-charge limited conditions: The cases in SEE[5] and TEE.[12–15] However, it is not generally correct for arbitrary values of SV. It is necessary to analyze the electrostatic structure in the sheath. The space-charge limited condition is given by the zero electric field on the material surface or at the bottom of the virtual cathode for both SEE and TEE.[16] The analytical calculation gives the space-charge limited current for cold ions $T_i=0$ as follows:

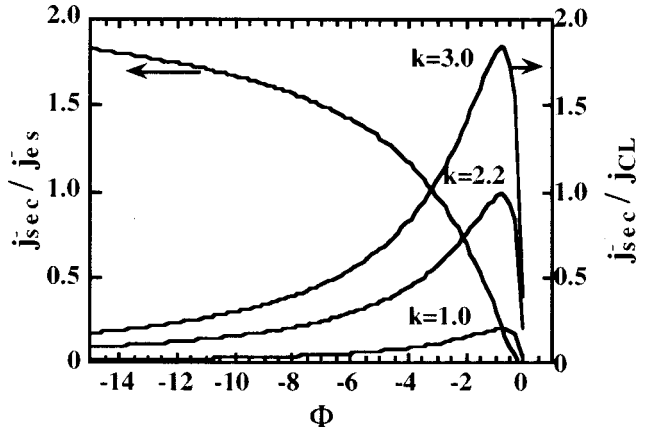

FIG. 5. Space charge limited current as a function of SV. It is compared with modified Child–Langmuir expressions with several sheath thicknesses.

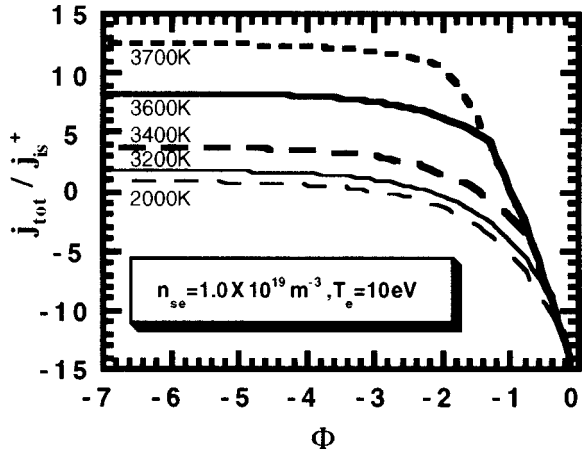

FIG. 6. Current-voltage characteristics for several surface temperatures of W plate, where correct space-charge limited current is considered.

$$j_{see}^{-}=\frac{(-\pi\Phi)^{1/2}g}{1+g}\,n_{se}e\left(\frac{2T_e}{\pi m_e}\right)^{1/2} \tag{5}$$

where

$$g=[-\beta_1+(\beta_1^2-4\beta_0\beta_2)^{1/2}]/(2\beta_2), \tag{6}$$

$$\beta_0=-4\Phi^2-2\Phi(e^{\Phi}-1)(e^{\Phi}-3),$$

$$\beta_1=4(1-2e^{\Phi})\Phi^2+8(e^{\Phi}-1)\Phi-(e^{\Phi}-1)^2, \tag{7}$$

$$\beta_2=4\Phi^2-8\Phi^3.$$

This is shown in Fig. 5 by thick solid line as a normalized form, where $j_{es}^{-}=en_{se}[8T_e/(\pi m_e)]^{1/2}/4$ is the random electron current, and is compared with the modified CL equation j_{CL} for several k values. Certainly, both values agree with each other for $k=2.2$ around $\Phi\sim 1$, corresponding to a floating voltage under the space-charge limited condition. Except at this point, the modified CL equation is found to overestimate the emission current.

When the emission current given by either SEE or the temperature-limited current

$$j_{em}^{-}=\gamma j_p \quad \text{or} \quad j_{em}^{-}=j_{Tht}^{-}=AT^2\,\exp\left(-\frac{e\phi_{\mathrm{W}}}{kT}\right), \tag{8}$$

is exceeded by the space-charge limited current, the emission current is given by Eq. (8) where A is Dushman's constant, T is the surface temperature, ϕ_w is the work function of the surface material, and γ is the ratio of the emission current to the primary electron current.

The ion current to the material surface is given by $j_i^{+}=n_{se}eMC_s$ where C_s is the sound speed expressed as $\{(T_e+T_i)/m_i\}^{1/2}$ (sometimes we assume $T_i=0$) and M is the Mach number given by the following expression: In the space-charge limited condition

$$M^2\geqslant(1+g)/[1+g/(2\Phi)]. \tag{9}$$

And in other cases, g should be replaced as follows:

$$g\rightarrow 0.5\gamma e^{\Phi}/\sqrt{-\pi\Phi}. \tag{10}$$

The total current is described by

$$\frac{j_{\mathrm{tot}}}{j_{is}^{+}}=-\frac{1-2(-\pi\Phi)^{1/2}ge^{-\Phi}}{1+g}\left(\frac{m_i}{2\pi m_e}\right)^{1/2}e^{\Phi}+\left(\frac{1+g}{1+g/(2\Phi)}\right)^{1/2}, \tag{11}$$

in the space-charge limited condition. And in other regions where we have the electron emission, the exchange given by Eq. (10) should be done. Of course, g should be zero when we have no electron emission. Figure 6 gives the current-voltage characteristics in the case of TEE.

C. Nonlinear bifurcation

We consider the system modeled as consisting of a uniform homogeneous plasma adjacent to the target plate heated to a sufficient temperature to emit thermoelectrons, which are accelerated across the sheath into the plasma. The magnetic field is normal to the surface, and the charged particles in the sheath is assumed to be collisionless. Power input P_h is introduced into the plasma cylinder with length L from the discharge region. The plasma electrons are assumed to obey the Boltzmann relation, and plasma ions are assumed to be cold. Thus, the SV is described by Eq. (2) where the emission current j_{em}^{-} is given by Eq. (5) or Eq. (8), depending on the space-charge condition. The plasma heat flow to the surface $Q=qS$ is determined mainly by the energy associated with impinged plasma particles, Eq. (1).

Plasma electrons have the power input P_h from the discharge region and also the energy input by injection of thermoelectrons accelerated from the surface into the plasma. On the other hand, they lose their energy by electron impact ionization and by escaping to the surface from the plasma. The radiation losses in the plasma is neglected here. The energy, $2T_e-e\phi$, is absorbed by the target plate. The time-dependent energy balance equation for electrons in the plasma is thus written

$$n_eV\frac{dT_e}{dt}=P_h-n_eVn_A\langle\sigma v\rangle_i e\phi_i-\phi j_{em}^{-}S$$

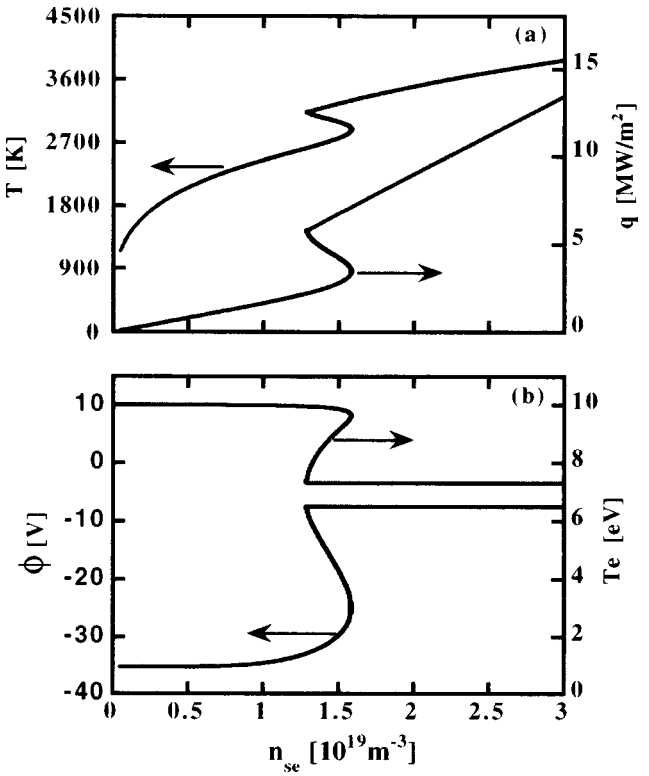

FIG. 7. Analytically obtained bifurcation S curves for W plate temperature T, plasma heat flux to the surface q, T_e and SV as a function of the He plasma density. $A=6.0\times10^5$ A/(m^2 K^2), $\phi_w=4.54$ eV, $\varepsilon=0.4$ and $R_{ie}=0.5$.

$$-\frac{(2T_e-e\phi)n_{se}}{4}S\left(\frac{8T_e}{\pi m_e}\right)^{1/2}e^{\Phi}. \tag{12}$$

The third term of the right-hand side is the energy input by injection of thermoelectrons into the plasma. Here V is the plasma volume ($V=SL$) and n_A is the neutral atom density.

The time evolution of the surface temperature is given by

$$HdT/dt=Q-\sigma\varepsilon 2ST^4-\phi_W j_{em}^- S-E_a j_a 2S, \tag{13}$$

where H is the heat capacity of the material, σ is the Stefan–Boltzmann constant, ε is the emissivity, j_a and E_a is the atomic flux and the energy due to material sublimation.

These energy balance equations for the plasma and the material are coupled with the equations for the floating voltage related to the emission current, so that we may have a series of hysteresis S curves typical for bifurcation as shown in Fig. 7, in which we have two states, hot and cold. Experimentally, we have a sudden jump in the W surface temperature and a drop in the sheath voltage even when we increase the plasma heat flow gradually in a continuous manner as shown in Fig. 8. When we decrease the plasma heat flow after the transition to the hot state, it continues to be kept even after the plasma condition returns to the state corresponding to the transition. In Fig. 8 the plasma density starts to decrease from $t=45$ min. We found that the central region of W sheet is melted down to make a hole.[14] Figure 7 shows that the plasma density at the sheath edge should be well above 1.5×10^{19} m^{-3} to have a transition. However, the

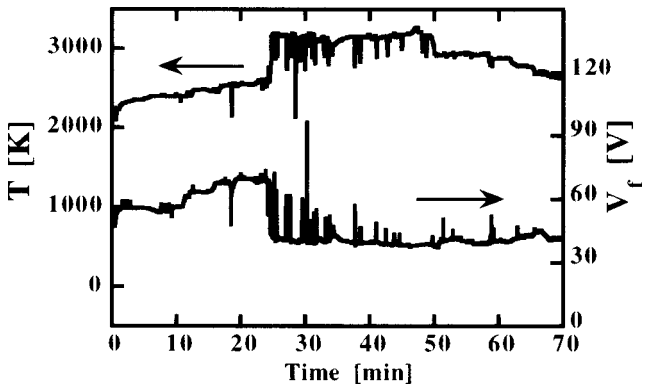

FIG. 8. The experimental results for plasma heat flow to W plate in He plasma. It is increased by increasing the source discharge current. At $t=24$ min, corresponding to $I_p=98$ A, $V_p=190$ V, $n_e=4.0\times10^{18}$ m^{-3}, the W plate is heated up to a temperature of 2600 K, sufficient for TEE, and a transition occurs. From $t=45$ min the plasma heat flow is decreased gradually in time.

maximum plasma density in the upstream, 20 cm from the target where we obtained Fig. 8, is at most 0.5×10^{19} m^{-3}, corresponding to below 0.3×10^{19} m^{-3} at the sheath edge. There would be more than a factor of 5 discrepancy between the zero-dimensional (0D) analysis and the experiment. It should be noted that a clear hysteresis S curve has been observed in a fundamental way by using a LaB_6-made emitting surface.[9,13]

D. Thermal contraction by cross-field plasma potential variation

The zero-dimensional analysis cannot explain an anomalous heat deposition, something like hot spot around the center.[17] We have to investigate these things carefully. We know that the energy transmission is very sensitive to the SV, especially on the low voltage side, which allows us to have an enormous electron energy flux. Sometimes, we have a substantial potential variation across the magnetic field in a plasma, while the conductive material has an equipotential all over the surface, so that we may have a very great variation of SV.[15] In our plasma device, a fairly deep hollow structure of plasma potential is created due to the PIG (Penning ionization gauge) configuration for plasma production, as shown in Fig. 9(b) where the normalized hollow potential is $\Phi_0=-10$ at the bottom. It results in the relatively low ϕ around the center having an excess electron heat flow, and the relatively high ϕ at the periphery having an increased ion heat flow, as shown in Fig. 9(b). When the plasma heat flow near the center is large enough to generate the thermoelectrons, the surface potential tends to decrease so that it may approach more closely to the plasma potential. This positive feedback makes the transition mentioned in the previous subsection have a very hot area near the center, as shown in Figs. 9 and 10, where the W sheet with the thickness of 0.1 mm is irradiated by the helium plasma, and the heat conduction on the surface is taken into account together with the heat balance Eq. (13) at every point over the surface. The space-charge limited current is correctly introduced here using Eq. (5). The critical density for the transition obtained by

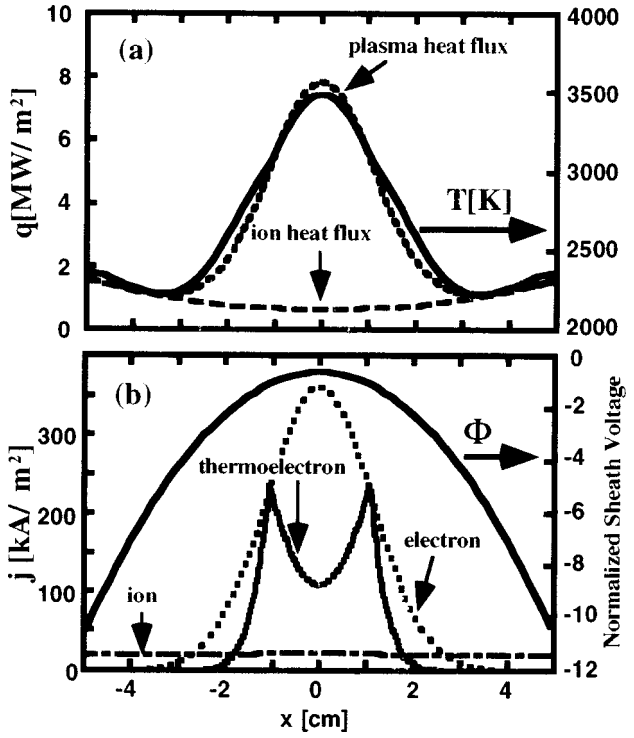

FIG. 9. Horizontal profiles of (a) the ion and total heat flux densities as well as the substrate temperature, and (b) the plasma ion and electron current densities, and TEE current density. $\Phi_0=-10$, $n_{se}=0.8\times10^{19}$ m^{-3} and $R_{ie}=0.5$.

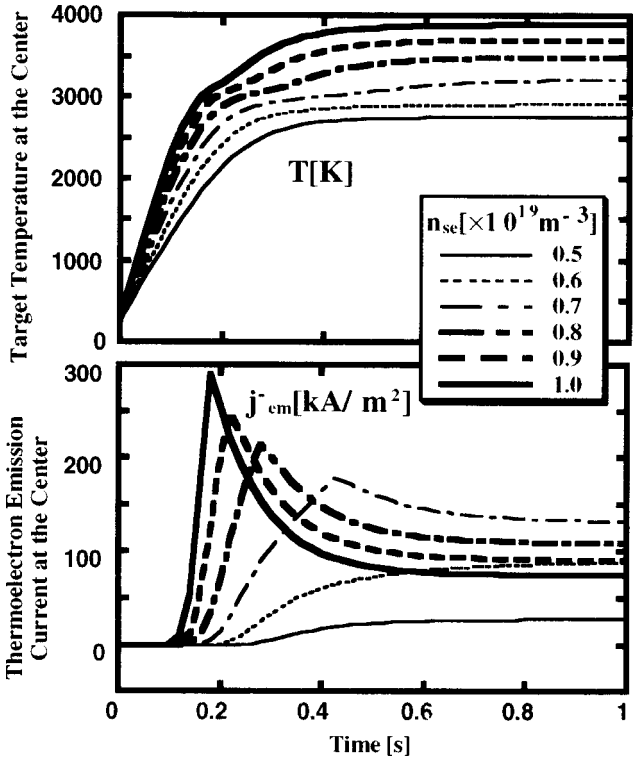

FIG. 10. Time evolutions of physical quantities under the same condition of Fig. 9.

the present one-dimensional (1D) model approaches the experimental value shown in Fig. 8, compared with the simple 0D analysis. The transition occurs at $n_{se}\sim0.8\times10^{19}$ m^{-3} in 1D model while 0D analysis needs $n_{se}\sim1.6\times10^{19}$ m^{-3}. The discrepancy still existing between the 1D model and the experiment may be explained by the change in material characteristics, such as work function, Dushman's constant, emissivity, etc., due to the modification of microstructure due to helium ion bombardment.[14]

IV. OTHER EFFECTS

A. Ion reflection

The ion reflection has a fairly important effect on δ, as described in Eq. (1). High Z materials, like W, have large R_{ie} for hydrogen isotopes and He. This has never been tested under the plasma environment in a fundamental way except in our experiment, carried out by target biasing over a wide range of normalized SV under a careful experimental conditions, where the plasma heat flow to the material was measured with a calibrated thermometer.[18]

A hydrogen or a helium bombardment on W gives a value of 0.46 or 0.43 for R_{ie}, respectively. They agree well with the values given by empirical formula.[19] On the other hand, in the carbon target case, experimental values of R_{ie} are by a factor of 2 larger than that of empirical formula. The reason for this difference is not understood fully, but the surface contamination by a small account of metal impurities might be one of the candidates. The hydrogen and oxygen contamination was excluded by the hot condition due to the plasma heat flow.

B. Ponderomotive forces

An rf-induced, directed force near the surface would modify sheath-presheath formations. Some reductions of plasma heat flow to the surface would be expected.[20] A transport barrier for electrons just in front of the surface makes the heat deposition profile on the divertor plate broad since the heat deposition width on the surface is proportional to the square root of the ratio of cross field to parallel transport coefficients.

1. Presheath modification[21]

We assume a uniform (PF) ponderomotive forces on electrons over the presheath region. That is, $eE^*=-d\psi/dx=$const. where $\psi=e^2\langle E_{\rm rf}^2\rangle/(2m_e\omega^2)$ is the PF potential. One-dimensional fluid theory with the momentum balance equation for isothermal ions, coupled with the modified Boltzmann relation, gives the plasma density as a function of M by introducing the intensity measure of PF $\alpha\equiv neE^*/m_iC_snn_A\langle\sigma v\rangle_i$. The numerator of the above definition is the force density on ions through electrons by PF, while the denominator is the ion momentum loss rate with the ion fluid velocity of C_s per unit volume per unit time by the ionization events. We get $n(M)/n_0=(1+\alpha M+M^2)^{-1}$, where n_0 is the plasma density at the stagnation point where $M=0$. If we assume $M=1$ at the sheath edge, then we obtain the sheath edge density, $n_{se}=n_0/(2+\alpha)$. The plasma density at the sheath edge decreases inversely proportional to α when α is large. The potential profile is obtained by inte-

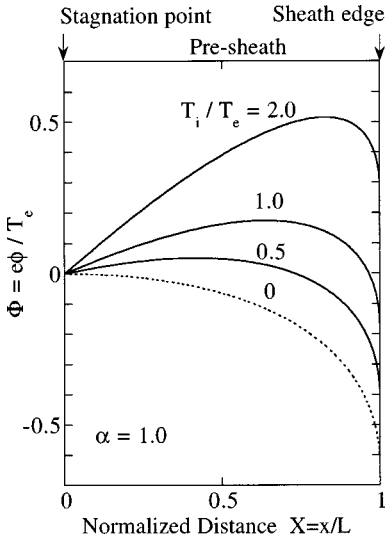

FIG. 11. Profiles of electrostatic potential over the presheath with $\alpha=1$ for several values of T_i/T_e.

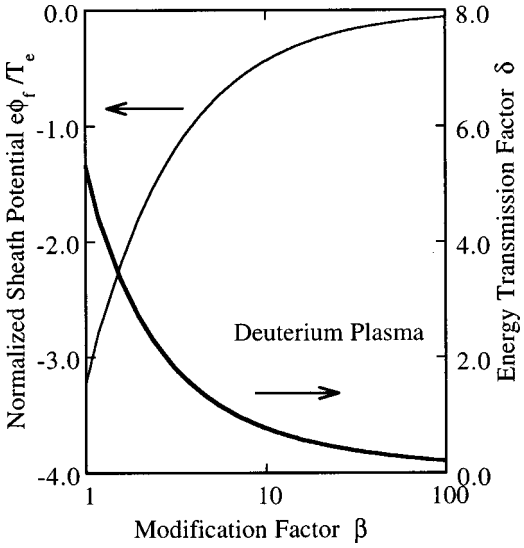

FIG. 12. Normalized sheath voltage and energy transmission factor as a function of the measure of PF, β. $T_i=0$ is assumed.

grating the modified electron momentum balance equation. The relation between M and the normalized distance $X=n_A\langle\sigma v\rangle_i x/C_s$ is obtained. Then, the presheath length is obtained by taking $M=1$. It is of the order of the so-called disturbance length, or collection length $C_s/n_A\langle\sigma v\rangle_i$. The potential structures over the presheath are shown in Fig. 11 for several values of T_i. If the electrons are reflected back by a strong PF, the ions should also be decelerated by the electrostatic potential, especially for warm ions, according to the charge neutrality in the presheath although the ion flow velocity at the sheath edge should be C_s.

Thus, the possibility of a strong reduction of the ion flux, therefore the plasma heat flow, on the material surface is demonstrated. Here, the ionic impact energy may also be decreased for reduction of sputtering by positively biasing the divertor plate, since the increase in electron heat flow by the positive biasing may be tolerable.

2. Sheath modification

The PF in rf sheath repels the electrons coming to the material surface. This has been really observed in the experiment on plasma-assisted bipolar arc,[22] in which the superposition of rf field on dc voltage makes the arc initiation voltage higher than that without rf.

In the following we attempt to include the effect of PF roughly in the conventional sheath theory. In order to have PF work well in the sheath, the rf excursion length of electrons should be smaller than the sheath width $\tilde{x}=eE_{\rm rf}/(m_e\omega^2)\leqslant k\lambda_{De}$. On the other hand, the ponderomotive potential should be high enough compared with the electron kinetic energy, that is, $\psi\geqslant T_e$. The above two conditions give an upper limit of plasma density for the effectiveness of PF in the sheath, $n_e\leqslant(k^2/2)(\varepsilon_0 m_e\omega^2/e^2)$. For example, if $f=2.45$ GHz and $k=5$, then $n_e\leqslant 10^{18}$ m^{-3}.

A collisionless free-fall theory for cold ions ($T_i=0$) is employed with an initial velocity at the sheath edge, $v_0=(2e|\phi_0|/m_i)^{1/2}$, where $\phi_0(<0)$ corresponds to the effective potential drop in the presheath. A modified Boltzmann relation $n_e(x)=n_{se}\exp[e\beta(\phi-\phi_0)/T_e]$ is assumed for electrons. The coefficient β corresponds to the multiplication factor of the potential on electrons coming from PF. An integration of Poisson's equation gives, when we assume $d\phi/dx=0$ at the sheath edge, the modified Bohm criterion including the reduced sound velocity $C_s^*:|\phi_0|\geqslant T_e/(2e\beta)$ or $v_0\geqslant\sqrt{T_e/(m_i\beta)}=C_s^*$. It is noted that the change in C_s by rf electric field is discussed in Ref. 23 by a different approach. Here, the electron kinetic motion decelerated by PF is the origin of reduction in C_s. The floating condition gives us the normalized SV, $\ln(\sqrt{2\pi m_e/(\beta m_i)})/\beta$. And then, δ becomes

$$\delta=\frac{q(\phi_{\rm sheath})}{T_e n_{se}\sqrt{T_e/m_i}}=-\frac{e\phi_{\rm sheath}}{T_e}\left(\frac{1}{\beta}\right)^{1/2}+\frac{1}{2}\left(\frac{8m_i}{\pi m_e}\right)^{1/2}\exp\left(\frac{e\beta\phi_{\rm sheath}}{T_e}\right). \tag{14}$$

Figure 12 shows the normalized SV and the energy transmission factor as a function of β. The strong PF substantially decreases the SV, resulting in a strong reduction of ion impact energy, as well as the electron heat flow to the surface.

We employ a simplified 1D formulation. A rectification effect or, in other words, self-biasing, is usually important but is not taken into account. However, a clear reduction of the particle flux into a surface on which rf voltage is applied is demonstrated experimentally as well as the transient increase just after turn-off of rf. They are explained by the above model.[24]

C. Anomalous energy transmission

It was postulated that the collision occurring inside the sheath, which are usually neglected, may be important in sheath formation,[25] because (1) oblique field angles extend sheath thickness to the scale of magnetic presheath; (2) high neutral densities are present near divertor surface at strike point due to recycling; and (3) shallow angles lead to long

path lengths through high density region, increasing number of collisions. Thus, δ would decrease according to the integrated neutral densities over the path length of ions and electrons through the sheath.

On the other hand, the divertor probe current-voltage characteristics become increasingly distorted away from the simple exponential during the high recycling and detached tokamak discharges. Under these collisional conditions, the ratio of the electron to ion saturation current is reduced and conventional single probe analysis overestimates the electron temperature. It is proposed that such an overestimation of Te due to the low electron to ion saturation current ratio may account for earlier observations of apparently low values of δ in DIII-D.[26] In the case of the joint European torus (JET)[27] experiments, one would infer from the probes that $\delta=8$ at low density and falls to $\delta=2$ to 3 under high recycling conditions.[28]

Such a reduction in the ratio of the electron to the ion saturation current has been observed for probes in our linear divertor plasma simulator NAGDIS-II to give a substantial overestimate of Te.[29,30] It means an apparent big reduction of δ even under the normal incidence of magnetic field on the material surface. Therefore, more careful studies are needed concerning the reduction of δ due to collisions inside the sheath.

V. CONCLUSIONS AND FUTURE WORKS

We have considered the energy transmission through plasma sheaths in a comprehensive way, taking several key physics factors into account. But, of course, there are several problems remaining to be solved. (1) Concerning the suppression of electron emission due to the electron gyromotion around the obliquely incident magnetic field, the formula for space-charge limited current across the magnetic presheath should be invoked. (2) The response of material facing the plasma should be considered self-consistently together with the cross-field heat transport when we have an electron emission.[31] A modification of material should be taken into account for the electron emission in a variety of conditions. (3) Detailed investigation would be needed to identify the reduction of δ due to collisions within the sheath for an obliquely incident magnetic field. (4) The energy transmission through the rf sheath to the rf antenna or Faraday screen is sometimes very important for heat deposition on these rf components. More detailed studies would be necessary.

ACKNOWLEDGMENTS

We would like to thank Professor M. Katsurai of University of Tokyo for his encouragement, Dr. K. Shiraishi of Hitachi Co. Ltd., Dr. S. Masuzaki of National Institute for Fusion Science, Dr. Y. Uesugi of Nagoya University for their contributions and discussions, and also S. Mizoshita, K. Kudose, and T. Shimada for their technical contributions.

[1] P. C. Stangeby, in *Physics of Plasma-Wall Interactions in Controlled Fusion*, edited by D. E. Post and R. Behrisch (Plenum, New York, 1986), p. 56.
[2] G. Janeschitz, K. Borrass, G. Feclerici, Y. Igitkhanov, A. Kukushkin, H. D. Pacher, G. W. Pacher, and M. Sugihara, J. Nucl. Mater. **220-222**, 73 (1995).
[3] G. F. Matthews, J. Nucl. Mater. **220-222**, 104 (1995).
[4] S. I. Krasheninnikov, A. Yu. Pigarov, D. A. Knoll, B. Labombard, B. Lipschultz, D. J. Sigmar, T. K. Soboleva, J. L. Terry, and F. Wising, Phys. Plasmas **4**, 1638 (1997).
[5] S. Takamura, S. Mizoshita, and N. Ohno, Phys. Plasmas **3**, 4310 (1996).
[6] K. Ohya, K. Nishimura, J. Kawata, and I. Mori, J. Nucl. Mater. **196-198**, 699 (1992).
[7] K. Shiraishi, N. Ohno, Y. Uesugi, and S. Takamura, J. Nucl. Mater. **196-198**, 745 (1992); K. Shiraishi, N. Ohno, and S. Takamura, J. Plasma Fusion Res. **69**, 1371 (1993).
[8] S. Mizoshita, K. Shiraishi, N. Ohno, and S. Takamura, J. Nucl. Mater. **220-222**, 488 (1995).
[9] S. Takamura, N. Ohno, K. Shiraishi, and S. Masuzaki, J. Nucl. Mater. **196-198**, 448 (1992).
[10] G. D. Hobbs and J. A. Wesson, Plasma Phys. **9**, 85 (1967).
[11] N. Ohno, E. Shimizu, and S. Takamura, Contrib. Plasma Phys. **36**, 386 (1996).
[12] S. Takamura and N. Ohno, in *Heat and Mass Transfer under Plasma Condition*, edited by P. Fauchais, M. Boulos, and J. Van der Mullen (Begell House, New York, 1995), p. 245.
[13] M. Y. Ye, S. Masuzaki, K. Shiraishi, S. Takamura, and N. Ohno, Phys. Plasmas **3**, 281 (1996).
[14] M. Y. Ye, S. Takamura, and N. Ohno, J. Nucl. Mater. **241-243**, 1243 (1997).
[15] T. Kuwabara, K. Kudose, M. Y. Ye, N. Ohno, and S. Takamura, Contrib. Plasma Phys. **36**, 349 (1998).
[16] G. D. Porter, Nucl. Fusion **22**, 1279 (1982).
[17] M. Z. Tokar, A. V. Nedospasov, and A. V. Yarochkin, Nucl. Fusion **32**, 15 (1992).
[18] S. Masuzaki, N. Ohno, and S. Takamura, J. Nucl. Mater. **223**, 286 (1995).
[19] W. Eckstein, Nucl. Fusion **1**, Suppl., 17 (1991).
[20] T. Shoji, A. Sagara, N. Noda, M. Hosokawa, K. Ida, H. Idei, H. Iguchi, O. Kaneko, S. Kubo, K. Matsuoka, S. Morita, K. Nishimura, S. Okamura, C. Takahashi, Y. Takeiri, and H. Yamada, J. Nucl. Mater. **196-198**, 824 (1992).
[21] S. Masuzaki and S. Takamura, Contrib. Plasma Phys. **34**, 318 (1994).
[22] Y. Shen, S. Takamura, G. Aoyama, and T. Okuda, Kakuyugo-Kenkyu, in Japanese **55**, 491 (1996).
[23] S. Takamura, S. Aihara, and K. Takayama, J. Phys. Soc. Jpn. **31**, 925 (1971).
[24] S. Masuzaki, N. Ohno, and S. Takamura, J. Nucl. Mater. **220-222**, 1112 (1995).
[25] A. H. Futch, G. F. Matthews, D. Buchenauer, D. N. Hill, R. A. Jong, and G. D. Porter, J. Nucl. Mater. **196-198**, 860 (1992).
[26] World Survey of Activities in Controlled Fusion Research [Nuclear Fusion special supplement 1994].
[27] See Ref. 26.
[28] R. D. Monk, A. Loarte, A. Chonkin, S. Clement, S. J. Davies, J. K. Ehrenbeng, H. Y. Guo, J. Lingentac, G. F. Matthews, M. F. Stamp, and P. C. Stangeby, J. Nucl. Mater. **241-243**, 396 (1997).
[29] N. Ezumi, N. Ohno, K. Aoki, D. Nishijima, and S. Takamura, ''Anomaly of Langumuir probe characteristics in detached recombining plasmas'' Contrib. Plasma Phys. (to be published).
[30] N. Ezumi, N. Ohno, Y. Uesugi, J. Park, S. Watanabe, S. A. Cohen, S. I. Krasheninnikov, A. Yu. Pigarov, M. Takagi, and S. Takamura, *Proceedings of the 24th EPS Conference on Controlled Fusion and Plasma Phys., Berchtesgaden* (European Physical Society, Petit-Lancy, 1997), Vol. 21A, Part III, p. 1225.
[31] K. Reinmuller and A. Bergmann, Proceedings of the 24th EPS Conference on Controlled Fusion and Plasma Phys., Berchtesgaden (European Physical Society, Petit-Lancy, 1997), Vol. 21A, Part IV, p. 1441.